Magnetic properties of the frustrated antiferromagnetic spinel $ZnCr_2O_4$ and the spin-glass $Zn_{1-x}Cd_xCr_2O_4$ ($x=0.05,0.10$)

H. Martinho, N. O. Moreno, J. A. Sanjurjo, and C. Rettori
Instituto de Física ''Gleb Wataghin,'' UNICAMP, 13083-970, Campinas-SP, Brazil

A. J. García-Adeva and D. L. Huber
University of Wisconsin-Madison, Madison, Wisconsin 53706

S. B. Oseroff
San Diego State University, San Diego, California 92182

W. Ratcliff II and S.-W. Cheong
Deptartment of Physics and Astronomy, Rutgers University, Piscataway, New Jersey 08854

P. G. Pagliuso and J. L. Sarrao
Los Alamos National Laboratory, Los Alamos, New Mexico 87545

G. B. Martins
National High Magnetic Field Laboratory, Florida State University, Tallahassee, Florida 32306
(Received 20 October 2000; revised manuscript received 5 February 2001; published 19 June 2001)

The T dependence ($2-400$ K) of the electron paramagnetic resonance (EPR), magnetic susceptibility $\chi(T)$, and specific heat $C_v(T)$ of the *normal* antiferromagnetic (AFM) spinel $ZnCr_2O_4$ and the spin-glass (SG) $Zn_{1-x}Cd_xCr_2O_4$ ($x=0.05,0.10$) are reported. These systems behave as a strongly frustrated AFM and SG with $T_N \approx T_G \approx 12$ K and -400 K$\gtrsim\Theta_{CW}\gtrsim -500$ K. At high-T the EPR intensity follows the $\chi(T)$ and the g value is T independent. The linewidth broadens as the temperature is lowered, suggesting the existence of short range AFM correlations in the paramagnetic phase. For $ZnCr_2O_4$ the EPR intensity and $\chi(T)$ decreases below 90 and 50 K, respectively. These results are discussed in terms of both nearest-neighbor Cr^{3+} ($S=3/2$) spin-coupled pairs and spin-coupled tetrahedral clusters with an exchange coupling of $|J/k|\approx 35-45$ K. The appearance of small resonance modes for $T\lesssim 17$ K, the observation of a sharp drop in $\chi(T)$ and a strong peak in $C_v(T)$ at $T_N=12$ K confirms, as previously reported, the existence of long range AFM correlations in the low-T phase. A comparison with recent neutron diffraction experiments, that found a near dispersionless excitation at 4.5 meV for $T\lesssim T_N$ and a continuous gapless spectrum for $T\gtrsim T_N$, is also given.

DOI: 10.1103/PhysRevB.64.024408 PACS number(s): 75.30.Kz, 75.40.−s, 75.50.Ee, 76.30.−v

I. INTRODUCTION

Frustration in the antiferromagnetic (AFM) ordering of fcc and spinel lattices was recognized long ago by Anderson in his analysis of the highly degenerate magnetic ground state of these structures.[1] This so-called *geometrical* frustration can prevent the system from undergoing spin-glass (SG) or AFM ordering down to temperatures much lower than the Curie-Weiss temperature $T_G, T_N \ll |\Theta_{CW}|$. It has also been shown, theoretically[2] and experimentally,[3] that the ground state degeneracy can be removed by atomic disorder leading to a SG type of ordering. The AFM *normal* spinel $ZnCr_2O_4$ structure, in which the octahedral Cr sites form a corner-sharing tetrahedra,[4] as well as the pyrochlore[5,6] and kagomé[7] structures, are excellent systems to study the *geometric* frustration phenomenon. $ZnCr_2O_4$ presents a very high Curie-Weiss temperature $\Theta_{CW}\approx -400$ K, and a first order AFM transition at $T_N\approx 12$ K (Ref. 8) accompanied by a slight tetragonal crystal distortion ($\Delta a/a\approx 10^{-3}$).[9] Besides, recent interesting low-T neutron diffraction experiments showed, in the ordered phase ($T\lesssim T_N$), the existence of a near dispersionless excitation at 4.5 meV, and for $T\gtrsim T_N$, a continuous gapless density of magnetic states.[10]

In this work we report on the T dependence ($2-400$ K) of the electron paramagnetic resonance (EPR), magnetic susceptibility $\chi(T)$, and specific heat $C_v(T)$, in a single crystal of the *normal* spinel $ZnCr_2O_4$ of cubic structure ($Fd\bar{3}m, O_h^7$) and in the Cd doped polycrystalline $Zn_{1-x}Cd_xCr_2O_4$ ($x=0.05,0.10$) compounds. A polycrystalline isomorphous compound of $ZnGa_2O_4$ was also used as a reference compound for the specific heat measurements.

II. EXPERIMENTAL DETAILS

Single crystals of $ZnCr_2O_4$ of typical size of $\sim 2\times 2\times 2$ mm^3 were obtained by the method of solid state reaction between stoichiometric amounts of Cr_2O_3 and ZnO in air.[11] The crystals show natural growing (001), (111), and (011) faces that were checked by the usual Laue method. Polycrystalline Cd doped $Zn_{1-x}Cd_xCr_2O_4$ ($x=0.05,0.10$) and $ZnGa_2O_4$ samples were prepared by the same method. The EPR experiments were carried out in a conventional ELEXSYS Bruker X-Band EPR spectrometers using a TE_{102} room temperature cavity. The sample temperature was varied

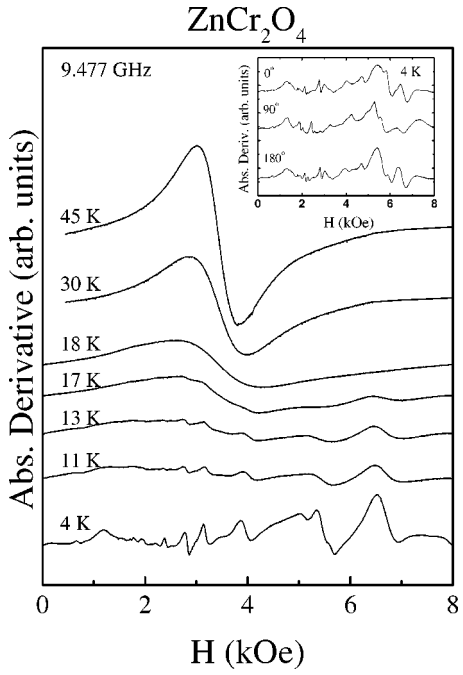

FIG. 1. T evolution ($4\ \mathrm{K} \leqslant T \leqslant 45\ \mathrm{K}$) of the EPR spectra for a $ZnCr_2O_4$ single crystal. The inset shows the spectra at $T=4$ K for different field orientations in the (110) plane.

by a temperature controller using a helium and nitrogen gas flux systems. This set up assures one that the spectrometer sensitivity remains about the same over a wide range of T. Magnetization measurements have been taken in a Quantum Design dc SQUID MPMS-5T magnetometer. The specific heat was measured using the heat pulse method in a Quantum Design calorimeter using the QD-PPMS-9T measurement system.

III. EXPERIMENTAL RESULTS

For the $ZnCr_2O_4$ single crystal, as the temperature is lowered from room-T, the EPR line broadens and its intensity goes through a maximum at about 90 K with no measurable resonance shift. Figure 1 shows the T evolution of the EPR spectra between 4 and 45 K. For $T \lesssim 17$ K the resonance distorts and small resonances modes emerge at low T. These modes do not depend on whether the EPR spectra are taken under field cooling (FC) or zero field cooling (ZFC) conditions. But, they depend on the size and shape of the sample and show a slight orientation dependence (see inset). For $T \gtrsim 20$ K the EPR spectra show a single isotropic resonance. For the Cd doped samples the resonance also broadens, but the intensity increases down to $T \approx 12$ K (see below) where, again, the resonance distorts and small resonance modes are seen. These modes also show the same spectra under FC and ZFC conditions.

Figure 2 shows the T dependence of the linewidth $\Delta H_{1/2}$ and g value between 18 and 400 K for the crystal of Fig. 1. The linewidth broadens at low-T, the g value is T independent and its value, $g=1.978(5)$, corresponds to the g value of Cr^{3+} ($3d^3$, $S=3/2$) in a cubic site.[12–15] Both, the g value and linewidth are isotropic for $T \gtrsim 20$ K. For the Cd doped

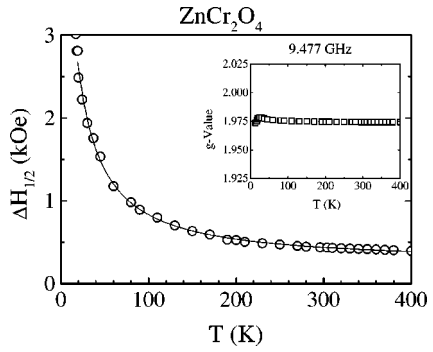

FIG. 2. T dependence ($18\ \mathrm{K} \leqslant T \leqslant 400\ \mathrm{K}$) of the EPR linewidth and g-value for the crystal of Fig. 1. The solid line shows the best fit of the linewidth to Eq. (1) (see text).

samples similar resonance line broadening and g values are obtained (not shown).

Figure 3 presents the dc magnetic susceptibility $\chi(T)$ corrected by the host diamagnetism in the range between 2 and 400 K for the same crystal of Fig. 1. FC and ZFC measurements at $H=2$ and 10 kOe gave no difference for the susceptibility data. At low field $\chi(T)$ shows the typical 3D AFM ordering with $\chi(T \to 0) \approx (2/3)\chi_{\max}$ ($T \approx 45$ K). The inset shows the sharp drop of the susceptibility at $T=12(1)$ K. This temperature defines the Néel temperature T_N for the 3D long range AFM ordering in $ZnCr_2O_4$. The inset shows that, for $T \lesssim T_N$, the susceptibility is field dependent, $\chi(T,H)$. This has been attributed to domain wall movement in the AFM ordered state.[17] The dotted line and solid line are fits to the data discussed in Sec. V.

Figure 4 compares the magnetic susceptibility of the $ZnCr_2O_4$ single crystal of Fig. 3 with those of the polycrystalline $Zn_{1-x}Cd_xCr_2O_4$ ($x=0.05,0.10$) samples. For $T \gtrsim 100$ K the data for the three compounds can be fitted to the usual Curie-Weiss law. The linear fit yields to an effective number of Bohr magnetons $\mu_{\mathrm{eff}}=3.95(10)\ \mu_B$, as expected for Cr^{3+} ($g=1.978$, $S=3/2$), and a Curie-Weiss temperature $\Theta_{\mathrm{CW}}=-390(20)$ K for $ZnCr_2O_4$. In a molecular field approximation $\Theta_{\mathrm{CW}}=-S(S+1)\ Jz/3k_B$. For S

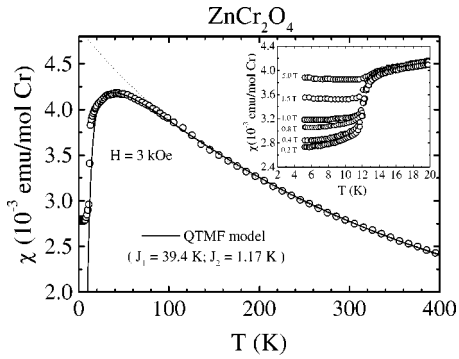

FIG. 3. T dependence ($2\ \mathrm{K} \leqslant T \leqslant 400\ \mathrm{K}$) of the magnetic susceptibility $\chi(T)$ at $H=3$ kOe (FC, ZFC). The inset shows the data for $2\ \mathrm{K} \leqslant T \leqslant 20$ K and $0.2\ \mathrm{T} \leqslant H \leqslant 5$ T. The dotted line is the Curie-Weiss approximation, and the solid line is the fit obtained using the quantum tetrahedral mean field model with $J_1=39.4$ K and $J_2=1.17$ K (see Sec. V).

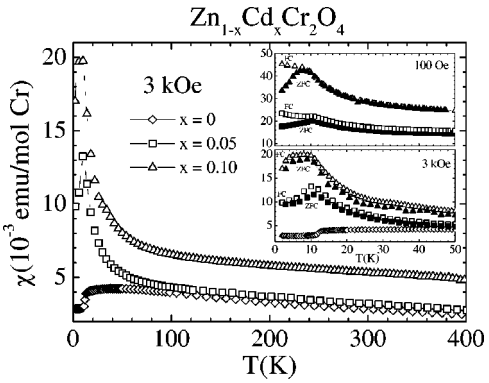

FIG. 4. T dependence ($2\ \mathrm{K} \leqslant T \leqslant 400\ \mathrm{K}$) of the FC magnetic susceptibility $\chi(T)$ at 3 kOe for $Zn_{1-x}Cd_xCr_2O_4$. The insets shows FC and ZFC data for $2\ \mathrm{K} \leqslant T \leqslant 50\ \mathrm{K}$ at $H = 100$ Oe and 3 kOe.

$= 3/2$, $z = 6$ (nearest neighbors), and $\Theta_{\mathrm{CW}} = -390$ K we obtain $J/k \approx 50$ K. The Curie-Weiss parameters for the $Zn_{1-x}Cd_xCr_2O_4$ ($x = 0.05, 0.10$) samples are given in Table I. For $T \lesssim 100$ K, Fig. 4 shows, however, that there is a significant difference between the pure and Cd doped compounds. Low (high) field ZFC-FC measurements show, in the Cd doped samples, the typical SG irreversibility (reversibility) for $T \lesssim T_G \approx 12$ K (see inset of Fig. 4). These results and the large values found for $|\Theta_{\mathrm{CW}}|$ (see Table I), clearly indicate that the Cd doped samples develop a highly frustrated SG-type behavior with $T_G \approx 12$ K.

Figure 5 presents the T dependence of the resonance intensity $I(T)$ for the $ZnCr_2O_4$ single crystal and the polycrystalline $Zn_{1-x}Cd_xCr_2O_4$ ($x = 0.05, 0.10$) samples. Using an EPR standard, we found that the intensity of the resonance at room-T, $I(300\ \mathrm{K})$, corresponds to the total amount of Cr^{3+} ions present in the samples. Similar to the susceptibility data shown in Fig. 4, here also we observe two T regimes, above and below $T \approx 100$ K. For $T \lesssim 100$ K $I(T)$ shows significant difference between the pure and Cd doped compounds. For the Cd doped samples we found that $I(T)$ and $\chi(T)$ correlate well above $T_G \approx 12$ K (not shown); however, for the pure sample this correlation is only observed for $T \gtrsim 100$ K (see inset in Fig. 5).

Figure 6 presents the T dependence of the specific heat $C_v(T)$ for the $ZnCr_2O_4$ single crystal, the polycrystalline $Zn_{1-x}Cd_xCr_2O_4$ ($x = 0.05, 0.10$) samples, and the reference compound $ZnGa_2O_4$. The inset show the strong effect that the Cd impurities have on the AFM transition of the pure compound $ZnCr_2O_4$. The large reduction in the peak of the $C_v(T)$ confirms the assignment of SG character for the transition observed at ≈ 12 K in the susceptibility data for the

TABLE I. Curie-Weiss parameters for $Zn_{1-x}Cd_xCr_2O_4$.

$Zn_{1-x}Cd_xCr_2O_4$	C (emu/mole Cr K)	θ_{CW} (K)	μ_{eff} (μ_B)
$x = 0.0$	1.95(2)	−390(20)	3.95(10)
$x = 0.05$	2.94(5)	−500(20)	4.85(20)
$x = 0.10$	2.57(5)	−483(20)	4.53(20)

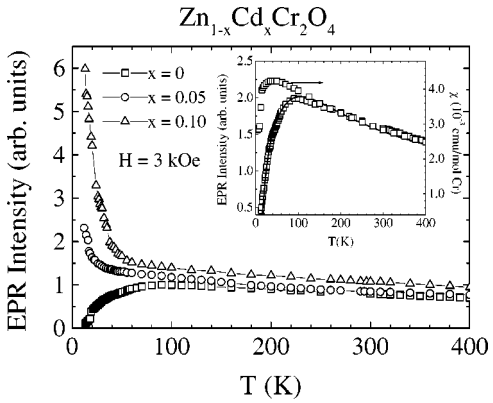

FIG. 5. T dependence ($15\ \mathrm{K} \leqslant T \leqslant 400\ \mathrm{K}$) of the EPR intensity $I(T)$ for $Zn_{1-x}Cd_xCr_2O_4$. The inset compares $I(T)$and $\chi(T)$ for $ZnCr_2O_4$ and the solid line is the best fit of $I(T)$ to Eq. (2) (see text).

Cd doped samples. The transition temperatures T_G and T_N are in fairly good agreement with those extracted from the susceptibility data (see inset in Fig. 4). Fields up to 9 T, within the data resolution, did not affect $C_v(T)$ and the AFM and SG transition temperatures.

IV. ANALYSIS AND DISCUSSION

The above EPR and magnetic susceptibility results show that the cubic *normal* spinel $ZnCr_2O_4$ and $Zn_{1-x}Cd_xCr_2O_4$ ($x = 0.05, 0.10$) compounds present interesting magnetic behavior between 2 K and 400 K. A high-T paramagnetic phase (HTPP), $T \gtrsim 100$ K for $ZnCr_2O_4$ and $T \gtrsim 12$ K for the Cd doped samples, and a low-T ordered phase (LTOP), $T \lesssim 12$ K, AFM for the pure and SG for the doped compounds. For $ZnCr_2O_4$, a transition between these two regimes is observed in the interval between 12 and 100 K. Our high-T EPR results are in general agreement with those already reported for polycrystalline samples.[12,14] However, the low-T EPR data for our $ZnCr_2O_4$ single crystal are quite different from those reported in Ref. 12. As the temperature decreases in the HTPP, the Cr^{3+} magnetic moments experience short range AFM correlations. The evidence for it is that, for $T \gtrsim 2T_N$, the EPR resonance shows no g shift and

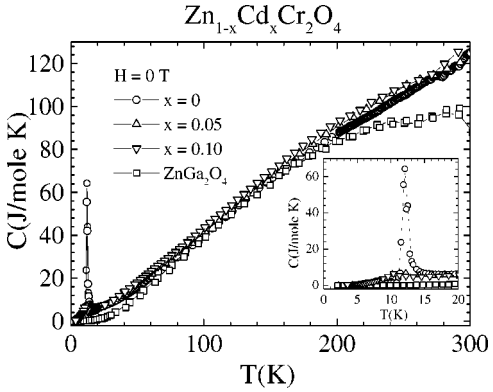

FIG. 6. T dependence ($2\ \mathrm{K} \leqslant T \leqslant 300\ \mathrm{K}$) of the ZF specific heat C_v/T for $Zn_{1-x}Cd_xCr_2O_4$ and $ZnGa_2O_4$. The inset shows C_v for $2\ \mathrm{K} \leqslant T \leqslant 20\ \mathrm{K}$.

a T dependence of the line broadening expected for a short range magnetic interaction in AFM materials above the Néel temperature T_N:[16]

$$\Delta H_{1/2}(T)-\Delta H_{1/2}(\infty)=\frac{R}{[T-T_N]^x}. \quad (1)$$

The solid line in Fig. 2 shows the fitting of the data to Eq. (1). The fitting parameters are $x=1.12(1)$, $T_N=12(1)$ K, $\Delta H_{1/2}(\infty)=250(10)$ Oe, and $R=110(20)$ Oe K^x. We should mention that, for $T\gtrsim T_N$, recent neutron diffraction measurements found a continuous gapless spectrum that was attributed to quantum critical fluctuations of small short range AFM correlated domains.[10] In the HTPP of $ZnCr_2O_4$, and for $T\gtrsim 100$ K, $\chi(T)$ and $I(T)$ follow the same T dependence (see inset in Fig. 5), indicating that all the Cr^{3+} ions that contribute to $\chi(T)$ also participate in $I(T)$. However, for $T\lesssim 100$ K, $\chi(T)$ deviates from $I(T)$, and they show maximums at $T\approx 40$ K and $T\approx 100$ K, respectively (see inset in Fig. 5). The maximum in $\chi(T)$ is caused by AFM correlations and indicates the onset of long range AFM ordering. Instead, in a first approximation, the maximum in $I(T)$ may be attributed to transitions within thermally populated excited states. The observation of EPR resonances in excited state levels of nearest-neighbor Cr^{3+} spin-coupled pairs diluted in the spinel $ZnGa_2O_4$ has been reported by Henning *et al.*[18] These authors were able to determine, from the observed $I(T)$, the energy separation between the first excited triplet state ($S=1$) and the ground singlet state ($S=0$) to be $|J/k|\approx 32$ K. Also, from the optical spectra of the Cr^{3+} spin-coupled pairs in $ZnGa_2O_4$ a value of ≈ 32 K was measured for $|J/k|$.[19] Within the same scenario and taking into account the thermal population of all the excited states for the Cr^{3+} spin-coupled pairs ($|\mathbf{S}_1+\mathbf{S}_2|$ - $|\mathbf{S}_1-\mathbf{S}_2|$; 3, 2, 1, and 0; $\mathbf{S}_1=\mathbf{S}_2=3/2$), the expected T dependence of the total EPR intensity $I(T)$ in the three excited states levels at energies J,3J, and 6J above the singlet ground state is given by[18]

$$I(T)\sim[A\exp(-J/kT)+B\exp(-3J/kT) + C\exp(-6J/kT)]/Z, \quad (2)$$

where $Z=1+3\exp(-J/kT)+5\exp(-3J/kT)+7\exp(-6J/kT)$ is the partition function, the coefficients A, B, and C are adjustable parameters proportional to the transition probability within each excited multiplet. The solid line in the inset of Fig. 5 shows the T dependence given by Eq. (2) for $A=10(2)$, $B=1(0.5)$, $C=4500(200)$, and $J/k=45(2)$ K. The value found for $|J/k|$ is larger than the one (≈ 32 K) found for isolated Cr^{3+} spin-coupled pairs in $ZnGa_2O_4$.[18] This difference is probably due to the different lattice parameters of $ZnCr_2O_4$ ($a=8.327$ Å) in $ZnGa_2O_4$ ($a=8.37$ Å).[15] Nevertheless, the value is in good agreement with that extracted from the Curie-Weiss temperature Θ_{CW} (see above).

As we pointed out elsewhere,[20] one can also attribute the difference between the temperature dependence of the susceptibility and the EPR intensity to the presence of nonresonant low frequency modes that contribute spectral weight to the Kramers-Kronig integral for the static susceptibility

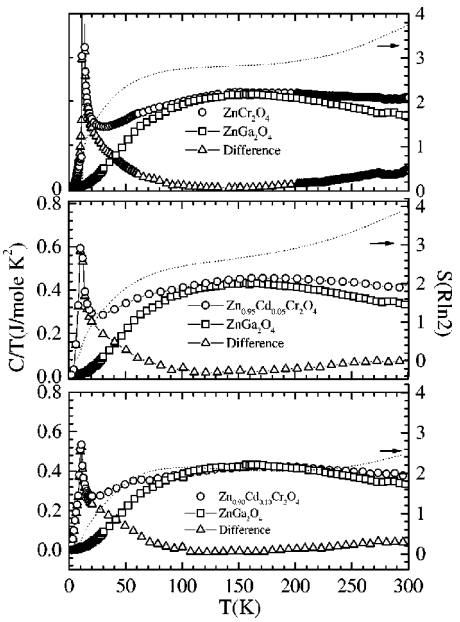

FIG. 7. T dependence ($2\ \text{K}\leqslant T\leqslant 300$ K) of the ZF C_v/T for $Zn_{1-x}Cd_xCr_2O_4$ and $ZnGa_2O_4$. The difference with the reference compound is also shown. The solid line gives the entropy per Cr pair S associated with the system's level multiplicity.

$$\chi(T)=\frac{2}{\pi}\int_0^\infty d\omega\frac{\chi''(\omega)}{\omega}, \quad (3)$$

but do not participate in the EPR absorption. It is likely that such modes are seen in inelastic neutron scattering above T_N.[10] The fact that the susceptibility and the EPR intensity have a common temperature variation in the Cd–doped samples suggests that the nonresonant, low frequency modes, if present, are not making a significant contribution to the susceptibility integral.

Figure 7 shows the C_v/T plots obtained from the data of Fig. 6 for each studied sample. The contribution from the magnetic component is obtained from the difference with the data for the non magnetic reference compound $ZnGa_2O_4$. The entropy per spin pair S is obtained integrating these differences and gives approximately the multiplicity of the involved levels $\approx 2^4=16$. Within the same scenario of Cr^{3+} spin-coupled pairs, the Schottky anomaly for the spin-coupled pairs is given by

$$\frac{C_v}{T}=\frac{R}{T}\frac{\partial}{\partial T}\left[T^2\frac{\partial \ln Z}{\partial T}\right]. \quad (4)$$

Figure 8 shows the fitting of the data to Eq. (4). The obtained value for $|J/k|=35(2)$ K suggests the scheme of levels shown in Fig. 8. The value found for $|J/k|$ is consistent with those values obtained independently from the Curie-Weiss temperature Θ_{CW} and EPR intensity measurements in the HTPP (see above). Also shown is the prediction of the quantum tetrahedral mean field model discussed in the following section.

In the LTOP our EPR experiments show the appearance of small resonance modes (see Fig. 1 for $T\lesssim 17$ K). We

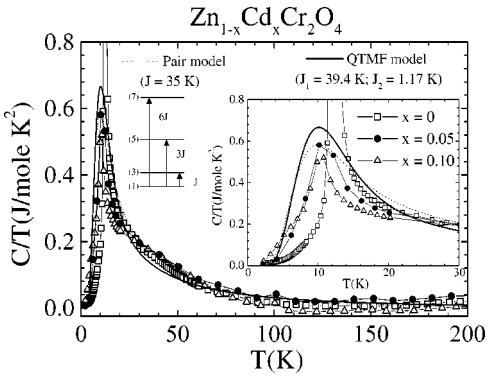

FIG. 8. T dependence ($2\ K \leqslant T \leqslant 300$ K) of the magnetic contribution to C_v/T. The dotted line is the Schottky anomaly calculated using Eq. (4) for a pair model of exchange coupled Cr^{3+} spins (see text). The solid line is the specific heat calculated from the quantum tetrahedral mean field model with $J_1 = 39.4$ K, the same value obtained from the fit of the susceptibility (see Sec. V).

believe that their sample size and shape dependence and angular variation are, probably, more related to demagnetizing effects rather than to the tetragonal crystal distortion observed at $T \approx 12$ K.[9] In addition for $T \lesssim T_N$ the magnetic susceptibility increases at higher fields (see inset of Fig. 3) and also, a small increase is oberved for $T \lesssim 5$ K (see Fig. 3). These behaviors are similar to those observed in magnetization measurements of polycrystalline samples of $ZnCr_2O_4$ and they have been attributed to the presence of AFM domains in the LTOP.[17] Thus, we associate our resonance modes with AFM domains that might be present in these materials as a consequence of their highly frustrated 3D long range AFM magnetic structure.

V. CONCLUSIONS

In conclusion, our EPR and $\chi(T)$ results in the *normal* spinel $ZnCr_2O_4$ show, between 12 and 100 K, a transition from a long to a short range regime of AFM correlations (LTOP-HTPP). From the T dependence of the EPR intensity in the HTPP an exchange parameter of $J/k \approx 45$ K between the Cr^{3+} ($S = 3/2$) spin-coupled pairs was extracted. This value is close to the one obtained independently from the Curie-Weiss temperature Θ_{CW} and from the Schottky anomaly observed in the specific heat. Thus, in a first approximation, the magnetic properties of these strongly frustrated systems in the HTPP can be described within a scenario involving just spin-coupling pairs of Cr^{3+} ($S = 3/2$). The sharp drop in $\chi(T)$ at $T \approx 12$ K, the peak in $C_v(T)$ also at $T \approx 12$ K, and the ordering temperature extracted from the broadening of the EPR linewidth ($T_N \approx 12$ K) confirmed the AFM ordering at $T \approx 12$ K in $ZnCr_2O_4$. The resonance modes observed in the LTOP and the field dependent susceptibility $\chi(T,H)$ indicates the presence of AFM domains in this material. Finally, we found that the disorder caused by the Cd impurities in $ZnCr_2O_4$ drives the system from an AFM to a SG type of highly frustrated magnetic ordering.

Although a model based on isolated pairs can account for many of the magnetic properties of $ZnCr_2O_4$, it does not include the interaction of the pairs with the surrounding ions. A widely used pair model that does include the effects of the interaction with neighboring spins is the constant coupling approximation.[21]. However, this model does not exploit the unique tetrahedral character of the Cr sublattice in $ZnCr_2O_4$. In particular, it predicts the same susceptibility for $ZnCr_2O_4$ as found in an unfrustrated simple cubic antiferromagnet, which has the same number of nearest-neighbor interactions (6) and exhibits a conventional AFM transition. This contradiction has led two of us (A.J.G.A. and D.L.H.) to develop a quantum tetrahedral mean field model.[22] In the quantum tetrahedral mean field approximation, the susceptibility per spin in the pyrochlore lattice (in units of $4\mu_B^2$) is expressed as

$$\chi^{\mathrm{TMF}} = \frac{\hat{\chi}^{\mathrm{tet}}(J_1,T)}{1+3(J_1+6J_2)\hat{\chi}^{\mathrm{tet}}(J_1,T)}, \tag{5}$$

where $J_1$and J_2 are the nearest and next-nearest-neighbor exchange integrals. The symbol $\hat{\chi}^{\mathrm{tet}}(J_1,T)$ denotes the susceptibility per spin of an isolated tetrahedron of spins and is written

$$\hat{\chi}^{\mathrm{tet}} = \frac{\sum_S g(S)S(S+1)(2S+1)e^{-J_1 S(S+1)/2T}}{12\sum_S g(S)(2S+1)e^{-J_1 S(S+1)/2T}}, \tag{6}$$

where the sum over S ranges from 0 to 6 in integer steps. The function $g(S)$ is the degeneracy factor, taking on the values 4, 9, 11, 10, 6, 3, and 1 for $S = 0$, 1, 2, 3, 4, 5, and 6, respectively.

In Fig. 3, we showed the data for the susceptibility in the paramagnetic phase together with the fits obtained using the quantum tetrahedral mean field model and the Curie-Weiss approximation, where $\chi^{\mathrm{CW}} = C/(T-\Theta)$. In the case of the tetrahedral analysis, the fit was obtained with $J_1 = 39.4$ K and $J_2 = 1.17$ K, whereas χ^{CW} was calculated with $\Theta = -388$ K. It is apparent there is excellent agreement between the data and the tetrahedral mean field approximation, which reproduces the peak in the susceptibility. In contrast, the susceptibility calculated in the Curie-Weiss approximation shows no peak, increasing monotonically with decreasing temperature.

The magnetic component of the specific heat can also be calculated with the quantum tetrahedral mean field model, provided the next-nearest-neighbor interactions are small, as is the case with $ZnCr_2O_4$. The specific heat is directly expressed in terms of the derivative of the internal energy with respect to temperature. The internal energy per spin is given by $U = 3J_1\langle \vec{S}_i \cdot \vec{S}_j \rangle$, where i and j are nearest neighbors. In the quantum tetrahedral mean field model $\langle \vec{S}_i \cdot \vec{S}_j \rangle$ is related to $\hat{\chi}^{\mathrm{tet}}$ through the equation

$$\langle \vec{S}_i \cdot \vec{S}_j \rangle = T\hat{\chi}^{tet} - S(S+1)/3, \tag{7}$$

where $S = 3/2$, in the case of $ZnCr_2O_4$. In Fig. 8, we compared the measured values of the magnetic specific heat with the predictions of the quantum tetrahedral mean field theory

using the value of J_1 inferred from the fit to the susceptibility. The agreement is seen to be very good. It is worth noting that the peak in the specific heat in the pair and tetrahedral cluster models, which is a short-range order effect, occurs at ~ 10 K, a value that is close to the critical temperature associated with the onset of long range order.

As noted, one of the unusual properties of the geometrically frustrated antiferromagnets is their sensitivity to small amounts of disorder. Such is the case here with the Cd-doped samples, where the AFM transition is replaced by a SG transition. Unlike the magnetically diluted system $ZnCr_{2-2x}Ga_{2x}O_4$,[3] where a fraction of the Cr ions are replaced by nonmagnetic Ga ions, the effect of the Cd substitution is to modify the Cr-Cr interaction in a random fashion, leading to bond disorder as opposed to the site disorder characterizing the Ga-doped samples. Unfortunately, there is as yet no theory for the bond disordered frustrated magnets that we can use to interpret our results.

ACKNOWLEDGMENTS

This work was supported by FAPESP Grants No 95/4721-4, 96/4625-8, 97/03065-1, and 97/11563-1São Paulo-SP, Brazil and NSF-DMR Grant No. 9705155 and NSF-INT No. 9602928, U.S. A.J.G.A. wants to thank the Spanish MEC for financial support under the Subprogramma General de Formación de Personal Investigador en el Extranjero.

[1] P.W. Anderson, Phys. Rev. **79**, 350 (1950); **79**, 705 (1950); **102**, 1008 (1956).
[2] L. De Seze, J. Phys. C **10**, L353 (1977); J. Villain, Z. Phys. B: Condens. Matter **33**, 31 (1979).
[3] D. Fiorani, S. Viticoli, J.L. Dormann, J.L. Tholence, J. Hammann, A.P. Murani, and J.L. Soubeyroux, J. Phys. C **16**, 3175 (1983); D. Fiorani, *ibid.* **17**, 4837 (1984).
[4] T.F.W. Barth and E. Posnjak, Z. Kristallogr. **82**, 325 (1932).
[5] R. Moessner and J.T. Chalker, Phys. Rev. Lett. **80**, 2929 (1998); R. Moessner, Phys. Rev. B **57**, R5587 (1998).
[6] B. Canals and C. Lacroix, Phys. Rev. Lett. **80**, 2933 (1998).
[7] A.P. Ramirez, G.P. Espinosa, and A.S. Cooper, Phys. Rev. B **45**, 2505 (1992).
[8] R. Plumier, M. Lecomte, and M. Sougi, J. Phys. (France) Lett. **38**, L149 (1977).
[9] F. Hartmann-Boutron, A. Gerard, P. Imbert, R. Kleibergerard, and F. Varret, C. R. Acad. Sci. Paris, Serie II Fascicule B **268**, 906 (1969); S.-H. Lee, C. Broholm, T.H. Kim, W. Rotcliff, S.-W. Cheong, and Q. Huang, (unpublished).
[10] S.-H. Lee, C. Broholm, T.H. Kim, W. Ratcliff, and S.-W. Cheong, Phys. Rev. Lett. **84**, 3718 (2000).
[11] Powder samples were prepared by the usual solid state reaction method starting with stoichiometric amounts of Cr_2O_3, ZnO, and CdO in air.
[12] M. Baran, S. Piechota, and A. Pajaczkowska, Acta Phys. Pol. A **59**, 47 (1981).
[13] D.E. O'Reilly and D.S. MacIver, J. Phys. Chem. **66**, 276 (1962).
[14] L. Forni and C. Oliva, J. Chem. Soc., Faraday Trans. 1 **84**, 2477 (1988).
[15] H. van den Boom, J.C.M. Henning, and J.P.M. Damen, Solid State Commun. **8**, 717 (1970).
[16] D.L. Huber, Phys. Rev. B **6**, 3180 (1972); M.S. Seehra, *ibid.* **6**, 3186 (1972); K. Kawasaki, Prog. Theor. Phys. **39**, 285 (1968).
[17] D. Fiorani and S. Viticoli, J. Magn. Magn. Mater. **49**, 83 (1985); L. Néel (unpublished).
[18] J.C.M. Henning, J.H. den Boef, and G.G.P. van Gorkom, Phys. Rev. B **7**, 1825 (1973).
[19] G.G.P. Gorkom, J.C.M. Henning, and R.P. van Stapele, Phys. Rev. B **8**, 955 (1973).
[20] H. Martinho, N.O. Moreno, J.A. Sanjuro, C. Rettori, A.J. García-Adeva, D.L. Huber, S.B. Oseroff, W. Ratcliff, II, S.-W. Cheong, P.G. Pagliuso, J.L. Sarrao, and G.B. Martins, J. Appl. Phys. (to be published).
[21] P.W. Kasteleijn and J.H. Van Kranendonk, Physica (Amsterdam) **22**, 317 (1956).
[22] A.J. García-Adeva and D.L. Huber, Phys. Rev. Lett. **85**, 4598 (2000).